Electronic Supplementary Information (ESI)

Rhodanine dye-based small molecule acceptors for organic photovoltaic cells

Yujeong Kim,[a] Chang Eun Song,[b] Sang-Jin Moon[c] and Eunhee Lim*[a]

[a] *Department of Chemistry, Kyonggi University, San 94-6, Iui-dong, Yeongtong-gu, Suwon-si, Gyeonggi 443-760, Republic of Korea*

[b] *Department of Materials Science and Engineering, KAIST, 373-1, Guseong-dong, Yuseong-gu, Daejon 305-701, Republic of Korea*

[c] *Korea Research Institute of Chemical Technology (KRICT), 100 Jang-dong, Yuseong-gu, Daejeon 305-600, Republic of Korea*

E-mail: ehlim@kyonggi.ac.kr

Contents

List of Figures

List of Tables

1. Materials and synthetic procedures

1.1 Materials

2-Bromo-5-formylthiophene, tetrakis(triphenylphosphine)palladium ($Pd(PPh_3)_4$), piperidine, and 1,2-dimethoxyethane (DME) were purchased from Aldrich. 3-Ethylrhodanine was purchased from TCI. All chemicals were used without further purification, and all reactions were performed under a nitrogen atmosphere with anhydrous solvents.

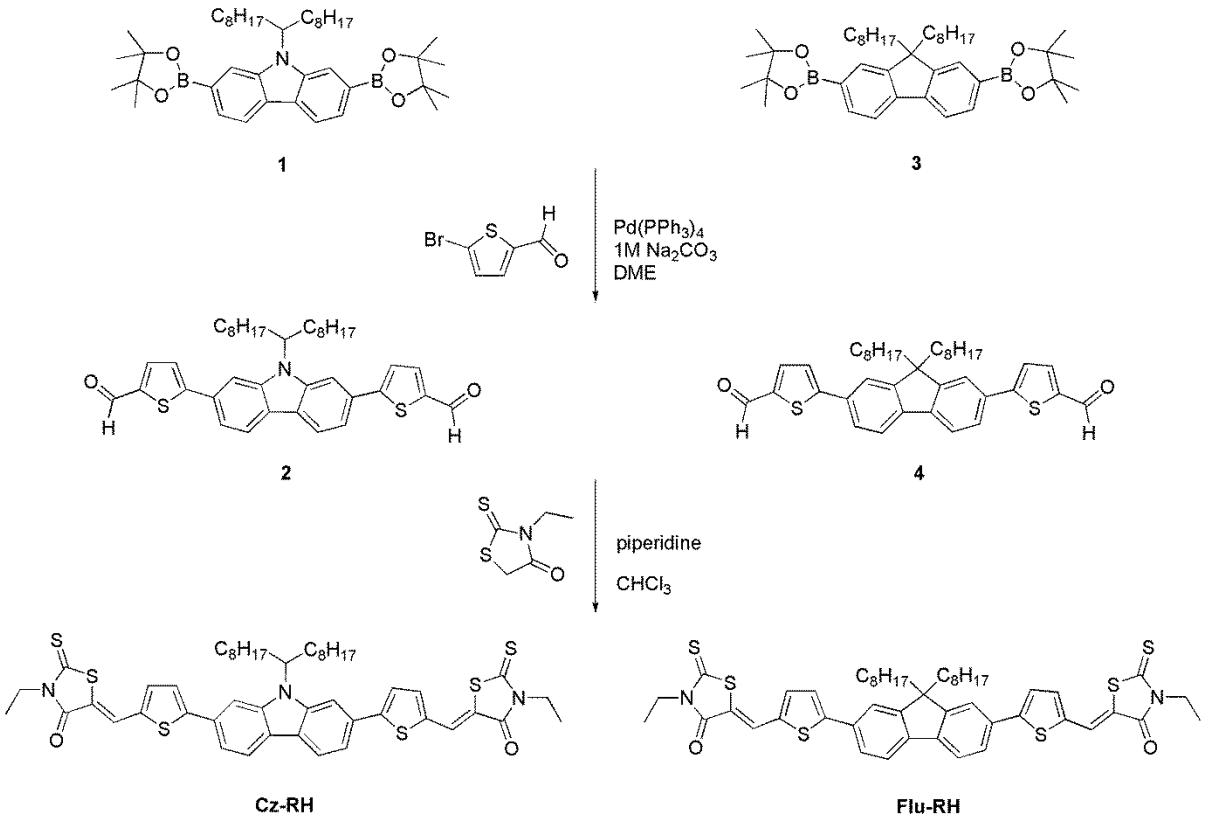

Scheme S1. Synthetic routes to **Cz-RH** and **Flu-RH**.

1.2 Synthesis of the small molecules

2,7-Bis(4′,4′,5′,5′-tetramethyl-1′,3′,2′-dioxaborolan-2′-yl)-N-9″-heptadecanylcarbazole (**1**) and 2,7-bis(4,4,5,5-tetramethyl-1,3,2-dioxaborolan-2-yl)-9,9-dioctylfluorene (**3**) were synthesized according to the literature.[1] Compounds **2** and **4** were synthesized using a palladium-catalyzed Suzuki coupling reaction between 2-bromo-5-formylthiophene and the compounds, **1** and **3**, respectively.[2] **Cz-RH** and **Flu-RH** were synthesized according to the publication to introduce 3-ethylrhodanine.[3]

*1.2.1 5,5′-(*N-9″-heptadecanylcarbazole-*2,7-diyl)bis(thiophene-2-carbaldehyde) (**2**)*

Compound **1** (1.0 g, 1.5 mmol) and $Pd(PPh_3)_4$ (0.088 g, 0.076 mmol) were put into a 2-neck round-bottom flask. A solution of 2-bromo-5-formylthiophene (0.87 g, 4.6 mmol) in DME (6.7 mL) and *aq*. Na_2CO_3 (4.9 mL, 1M) were injected into the mixture under nitrogen. After stirring at reflux refluxed for 4 h, the reaction was cooled to room temperature and water (20 mL) was added. The mixture was extracted with dichloromethane and water. The collected organic layer was dried over $MgSO_4$. After removing the solvent under reduced pressure, the crude product was recrystallized from dichloromethane/petroleum ether (6.0 mL/60 mL) to give the product as yellow powder (0.75 g; yield: 79%). ^{1}H NMR ($CDCl_3$, 400MHz): δ 9.95 (s, 2H), 8.14 (dd, 2H), 7.90 (s, 1H), 7.81 (d, 2H), 7.72(s, 1H), 7.60 (d, 2H), 7.54 (d, 2H), 4.64 (m, 1H), 2.34 (m, 2H), 2.02 (m, 2H), 1.18 (m, 24H), 0.81 (t, 6H). (The multiple proton peaks are due to atropisomerism)[4]

*1.2.2 5,5'-(9,9-dioctyl-9H-fluorene-2,7-diyl)bis(thiophene-2-carbaldehyde) (**4**)*

Compound **4** was prepared in the same manner as **2** using compound **3** (1.0 g, 1.6 mmol), $Pd(PPh_3)_4$ (0.088 g, 0.090 mmol), and a solution of 2-bromo-5-formylthiophene (0.90 g, 4.7 mmol) in DME (6.8 mL) and *aq*. Na_2CO_3 (5.1 mL, 1M), resulting in yellow powder (0.79 g; yield: 83%). ^{1}H NMR ($CDCl_3$, 400MHz): δ 9.94 (s, 2H), 7.80 (d, 2H), 7.79 (d, 2H), 7.72 (dd, 2H), 7.66 (s, 2H), 7.51 (d, 2H), 2.06 (m, 4H), 1.14 (m, 20H), 0.81 (t, 6H), 0.69 (m, 4H).

*1.2.3 2,2'-((5,5'-(*N-9″-heptadecanylcarbazole-*2,7-diyl)bis(thiophene-5,2-diyl))bis(methanylylidene))-bis(3-ethyl-2thioxothiazolidin-4-one)) (**Cz-RH**)*

Three drops of piperidine were added to a solution of **2** (0.58 g, 0.93 mmol) and 3-ethylrhodanine (1.5 g, 9.3 mmol) in chloroform (30 mL). The resulting solution was stirred at reflux for 24 h and then poured into cold water. The mixture was extracted with dichloromethane and water. The collected organic layer was dried over $MgSO_4$. After removing the solvent under reduced pressure, the crude product was purified by silica gel chromatography using chloroform as an eluent and then recrystallized from hexane and chloroform two times to give the product as red powder (0.60 g; yield: 71%). ^{1}H NMR ($CDCl_3$, 400MHz): δ (ppm) 8.14 (m, 2H), 7.93(s, 2H), 7.67-7.86 (m, 2H), 7.59 (d, 2H), 7.53 (br, 2H), 7.48(d, 2H) 4.69 (m, 1H), 4.25 (m, 4H) 2.38 (m, 2H), 2.05 (m, 2H), 1.15-1.39 (m, 28H), 0.80 (m, 8H). (The multiple proton peaks are due to atropisomerism)[4] ^{13}C NMR ($CDCl_3$, 100MHz): δ (ppm) 192.12, 167.32, 153.86, 143.19, 139.82, 136.98, 135.64, 131.14, 130.68, 125.40, 124.80, 124.27, 122.90, 121.29, 121.04, 120.34, 117.83, 117.65, 108.86, 106.31, 56.87, 39.96, 33.92, 31.76, 29.43, 29.34, 29.21, 26.82, 22.60, 14.07, 12.33. (The multiple proton peaks are due to atropisomerism)[4] Anal. Calcd for $C_{49}H_{57}N_3O_2S_6$: C, 64.50; H, 6.30; N, 4.61; O, 3.51; S, 21.09. Found: C, 64.65; H, 6.13; N, 4.31; S, 21.02.

*1.2.4 2,2'-((5,5'-(9,9-Dioctyl-9H-fluorene-2,7-diyl)bis(thiophene-5,2-diyl))bis(methanylylidene))-bis(3-ethyl-2thioxothiazolidin-4-one)) (**Flu-RH**)*

This compound was prepared in the same manner as **Cz-RH** using compound **4** (0.50 g, 0.82 mmol) and 3-ethylrhodanine (1.3 g, 8.2 mmol) in chloroform (32 mL) to give orange powder (0.52 g; yield: 70%). ^{1}H NMR ($CDCl_3$, 400MHz): δ (ppm) 7.92 (s, 2H), 7.78 (d, 2H), 7.71 (dd, 2H), 7.62 (m, 2H), 7.51 (d, 2H), 7.46 (d, 2H), 4.25 (m, 4H), 2.10 (m, 4H), 1.34 (m, 8H), 1.17 (m, 14H), 0.80 (m, 8H), 0.68 (m, 6H). ^{13}C NMR ($CDCl_3$, 100MHz): δ (ppm) 192.10, 167.36, 153.11, 152.29, 141.45, 136.99, 135.58, 132.37, 125.34, 125.29, 124.73, 120.75, 120.53, 120.15, 55.64, 40.29, 39.97, 31.77, 29.89, 29.18, 23.79, 22.60, 14.07, 12.33. Anal. Calcd for $C_{49}H_{56}N_2O_2S_6$: C, 65.58; H, 6.29; N, 3.12; O, 3.57; S, 21.44. Found: C, 65.70; H, 5.92; N, 2.89; S, 20.60.

2. Physical measurements

NMR spectra were recorded on a Bruker AVANCE II 400 spectrometer. Elemental analyses were performed with a Flash EA 1112 series from Thermo Electron Corporation. DSC was performed on a TA instrument Q100 at heating and cooling rates of 10 ^{o}C/min under a nitrogen atmosphere. TGA was performed under a nitrogen atmosphere at a heating rate of 10 ^{o}C/min using a Perkin Elmer TGA7 thermogravimetric analyzer. UV-vis and PL spectra were obtained using a Shimadzu UV-2550 and a Perkin Elmer LS-55 fluorescence spectrometers. The oligomer and blend films used in the UV-vis and PL measurements were prepared by spin coating from solution. The optical energy band gaps (E_g) were estimated from the absorption onset wavelengths (E_g = 1240/ λ_{onset} (eV)) of the oligomer films (*o*-DCB). The electrochemical properties of the oligomers were studied by cyclic voltammetry (CV) with a BAS 100B electrochemical analyzer. A three electrode system was used and consisted of a non-aqueous reference electrode (0.1 M Ag/Ag^+ acetonitrile solution), a platinum working electrode, and a platinum wire as a counter electrode. The redox potential of the oligomers was measured in acetonitrile with 0.1 M (n-$C_4H_9)_4N$-PF_6. The films were prepared by dip-coating the oligomer solution onto the platinum working electrode, and the measurements were calibrated using the ferrocenium/ferrocene redox value of –4.8 eV as an external reference. The highest occupied molecular orbital (HOMO) and lowest unoccupied molecular orbital (LUMO) energy levels were estimated according to the empirical relationship proposed by Leeuw et al. (I_p(HOMO) = –($E_{onset,ox}$ + 4.39) (eV) and I_p(LUMO) = –($E_{onset,red}$ + 4.39) (eV), where $E_{onset,ox}$ and $E_{onset,red}$ are the onset potentials of oxidation and reduction, respectively).[5] The LUMO level of PCBM, measured at the same time, was –3.82 eV. AFM images were obtained with a Scanning Probe Microscope (XE-100) by Park Systems. The AFM measurements were performed on the same samples that were used in the OPV devices as the top layer of the device (ITO/PEDOT:PSS/P3HT:acceptor).

3. Fabrication of the OPV devices

PCBM and PEDOT:PSS (Clevios P VP AI 4083) were purchased from EM Index and Heraeus, respectively. In this study, we fabricated the devices with a conventional structure of ITO/PEDOT:PSS/P3HT:oligomer or PCBM/LiF/Al, where P3HT was used as an electron donor, and the oligomer and PCBM were used as an electron acceptor. The ITO glass was cleaned with sequential ultrasonic treatment in detergent, deionized water, acetone, and isopropyl alcohol for 15 min each and subsequently dried in an oven for 5 h. The ITO-coated glass substrates were pre-treated in a UV-ozone oven for 15 min. A layer of PEDOT:PSS (~30 nm) was spin-coated on top of the ITO-coated glass substrates. The BHJ active layers were spin-cast at 3000 rpm from a solution of P3HT and oligomer in chloroform and *o*-DCB at a total solids concentration of 15 mg mL^{-1} and 40 mg mL^{-1} respectively. The average thickness of the active layers using chloroform (~100 nm) and *o*-DCB (~200 nm) were measured with an Alpha-Step IQ surface profiler. A LiF (~0.5 nm) and an Al (~100 nm) layer were directly deposited on the active layer under a vacuum of ~10^{-6} Torr. The effective area of all devices was measured to be 9 mm^2. The *I-V* curves of the devices were measured using a computer-controlled Keithley 236 source measure unit. The characterization of un-encapsulated solar cells was carried out in air under AM 1.5G illumination, 100 mW cm^{-2}, using a xenon lamp-based solar simulator. The simulator irradiance was characterized using a calibrated spectrometer, and the illumination intensity was set using an NREL-certified silicon diode with an integrated KG1 optical filter. The EQE was measured using a reflective microscope objective to focus the light output from a 100 W halogen lamp outfitted with a monochrometer and an optical chopper (PV Measurements, Inc.). The photocurrent was measured using a lock-in amplifier, and the absolute photon flux was determined using a calibrated silicon photodiode.

4. ^{1}H and ^{13}C NMR spectra

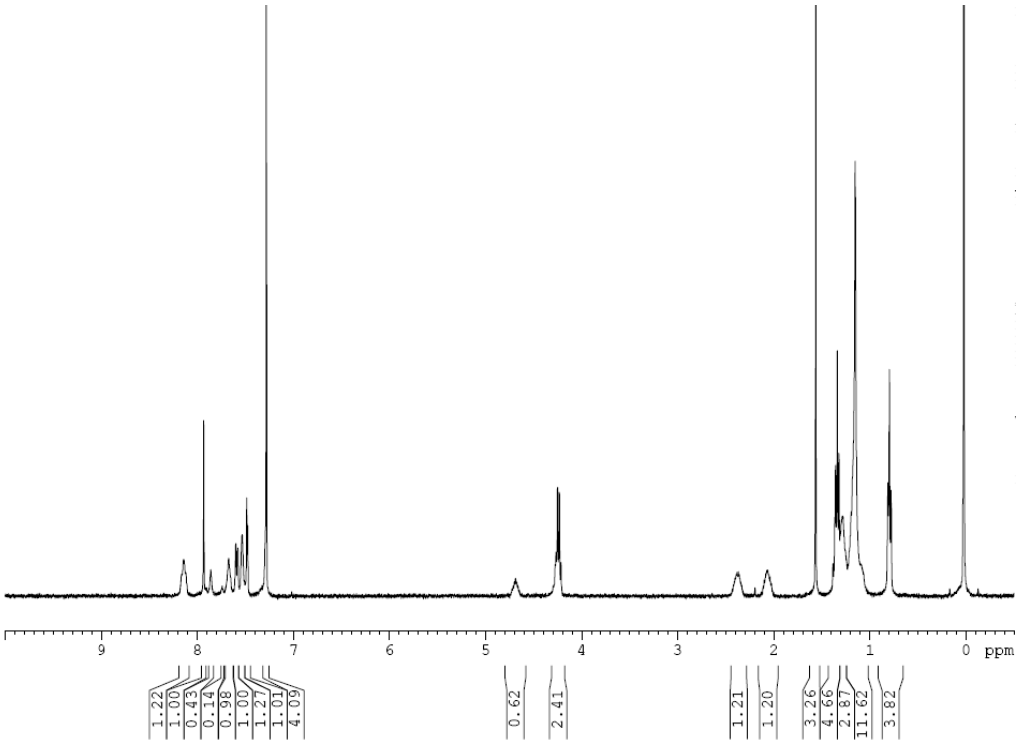

Figure S1. ^{1}H NMR spectra of **Cz-RH**.

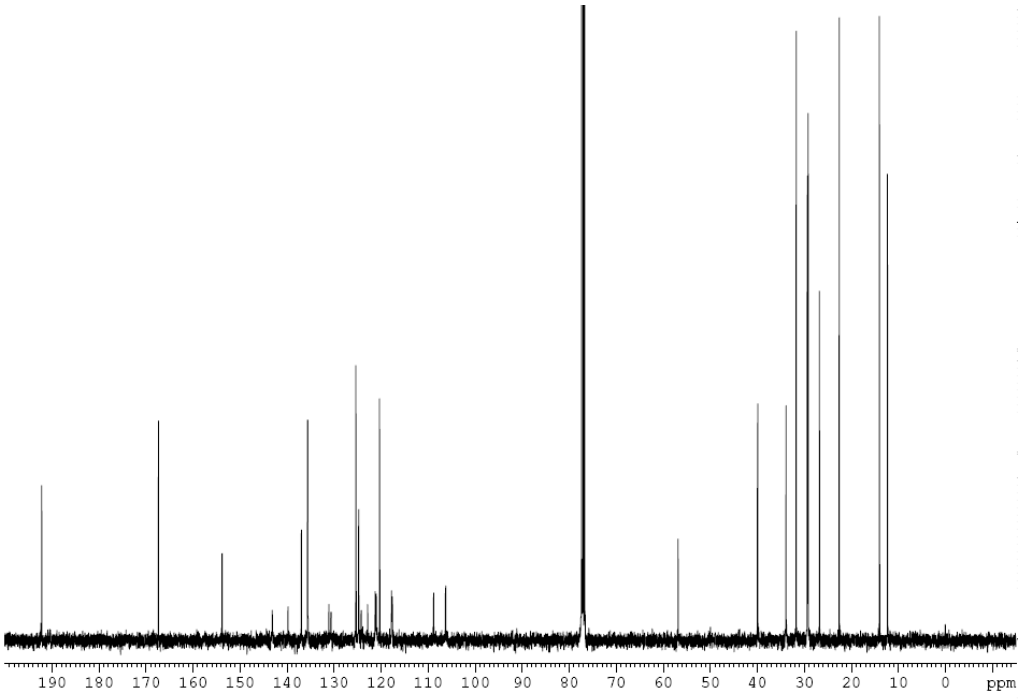

Figure S2. ^{13}C NMR spectra of **Cz-RH**.

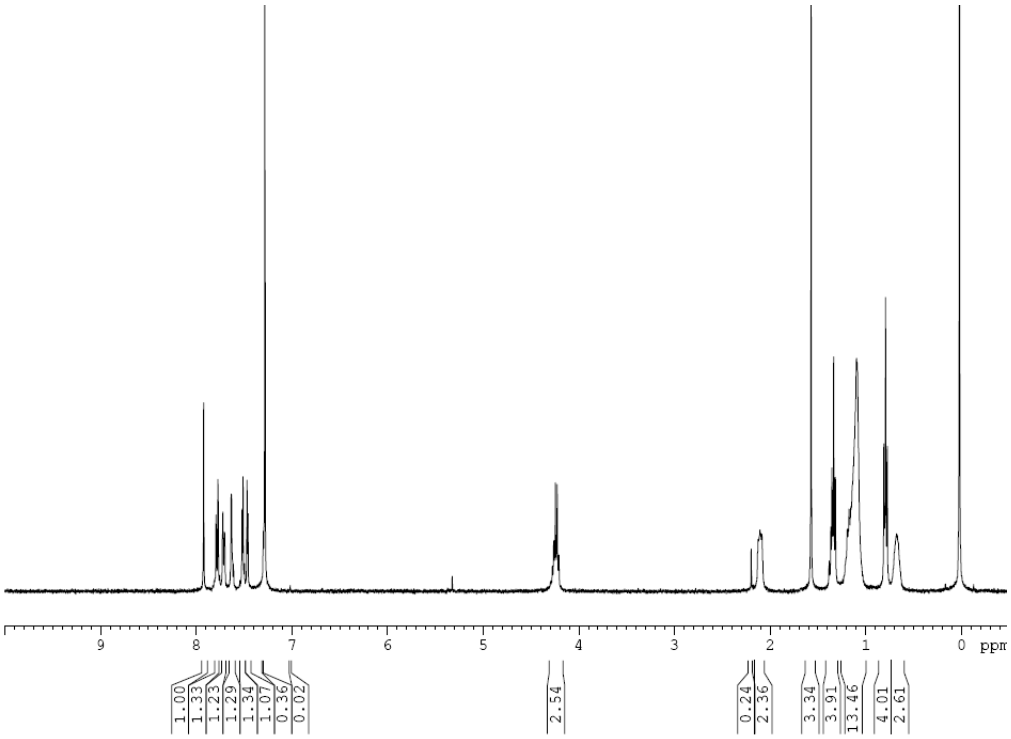

Figure S3. ^{1}H NMR spectra of **Flu-RH**.

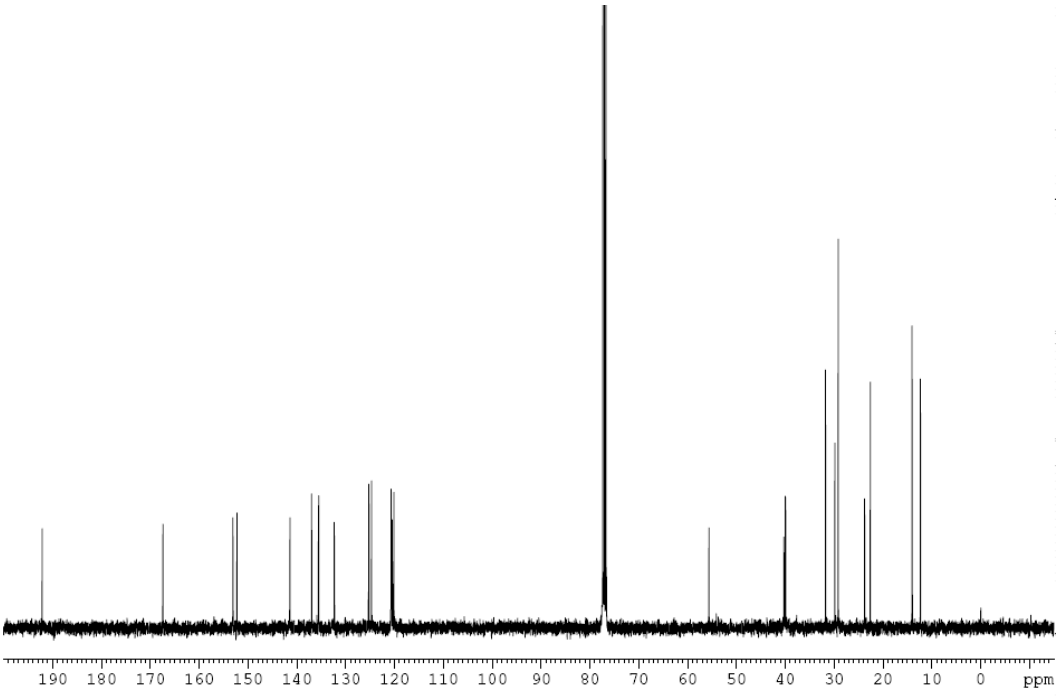

Figure S4. ^{13}C NMR spectra of **Flu-RH**.

5. Differential scanning calorimetry (DSC) and thermogravimetric analysis (TGA) spectra

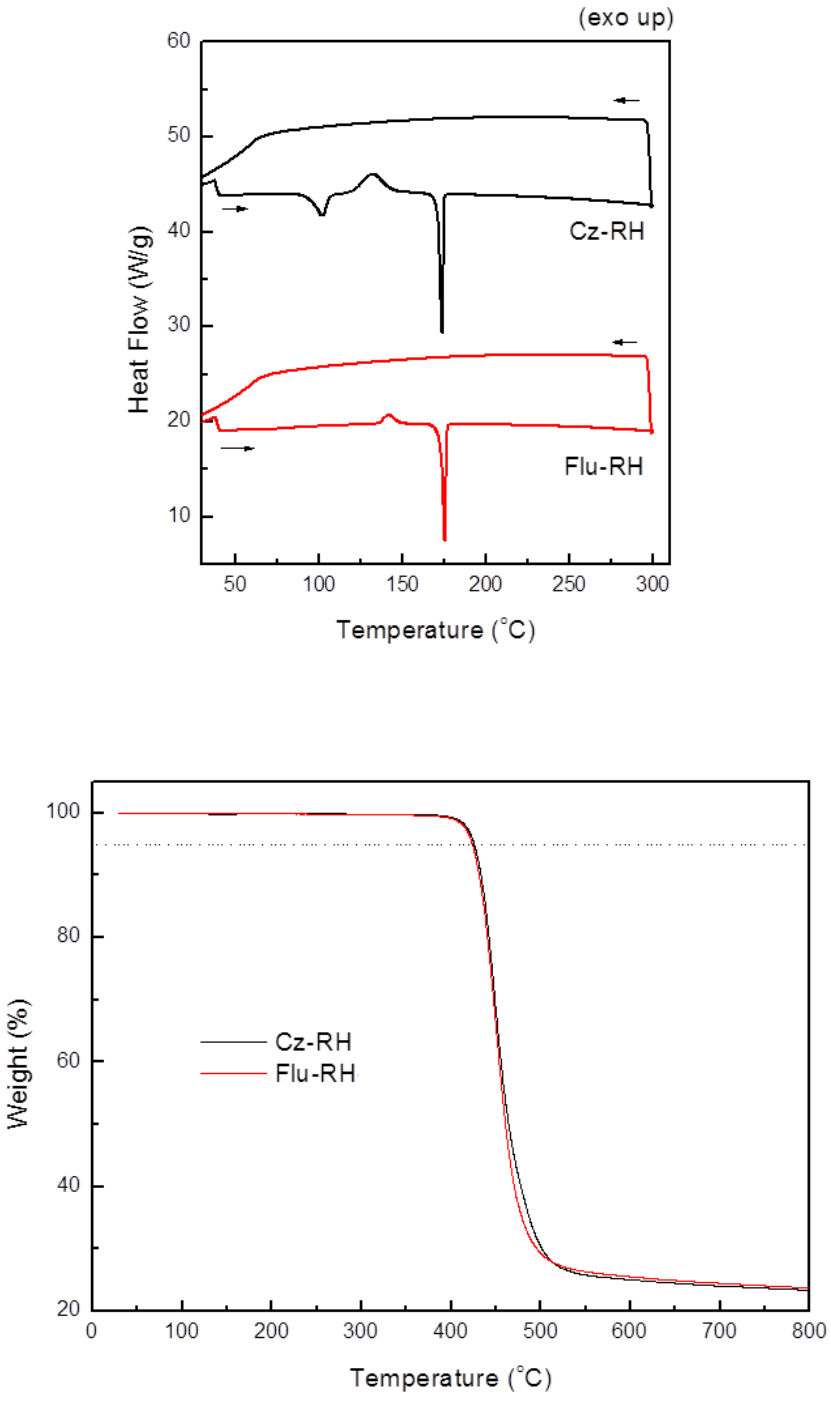

Figure S5. DSC (top) and TGA (bottom) curves of **Cz-RH** and **Flu-RH**.

6. OPV characteristics

Table S1. Photovoltaic performances of the OPVs based on P3HT:**Cz-RH** with different solvents, blend ratios and annealing temperatures.

		D:A Ratio	Annealing Temp [°C][a]	V_{OC} [V]	J_{SC} [mA/cm^2]	*FF* [%]	PCE [%]
Cz-RH	*o*-DCB	1:0.5	80	0.93	3.50	40	1.30
		1:0.5	100	0.98	3.77	42	1.54
		1:0.5	120	0.98	3.58	43	1.49
		1:1	W/O	0.92	4.46	43	1.76
		1:1	90	0.98	5.17	46	2.36
		1:1	120	0.94	4.42	44	1.83
		1:1	150	0.96	4.19	44	1.78
		1:1.5	80	1.03	4.82	50	2.50
		1:1.5	100	1.03	4.69	53	2.56
		1:1.5	120	1.03	4.63	50	2.40
	CF	1:0.5	90	1.11	1.13	47	0.59
		1:0.5	120	1.10	1.24	50	0.68
		1:0.5	150	1.07	1.48	50	0.79
		1:1	90	1.07	1.17	41	0.51
		1:1	120	1.10	1.27	49	0.69
		1:1	150	1.08	1.44	47	0.74
		1:2	90	1.09	1.45	40	0.63
		1:2	120	1.08	1.38	42	0.63
		1:2	150	1.07	1.44	42	0.65
	CB	1:1	W/O	1.05	2.27	32	0.77
		1:1	90	1.06	2.38	33	0.83
		1:1	120	1.05	2.08	37	0.81
		1:1	150	1.05	2.20	41	0.94

[a] Annealed for 10 min.

Table S2. Photovoltaic performances of the OPVs based on P3HT:**Flu-RH** and P3HT:PCBM with different solvents, blend ratios, and annealing temperatures.

		D:A Ratio	Annealing Temp [°C][a]	V_{OC} [V]	J_{SC} [mA/cm^2]	FF [%]	PCE [%]
Flu-RH	*o*-DCB	1:1	W/O	0.96	4.81	43	2.01
		1:1	90	1.01	5.22	48	2.53
		1:1	120	1.04	5.44	51	2.89
		1:1	150	1.04	5.29	50	2.78
		1:1	180	1.00	4.03	39	1.56
		1:1.5	80	1.03	5.61	51	2.95
		1:1.5	100	1.03	5.70	52	3.08
		1:1.5	120	1.03	5.52	53	3.00
		1:1.5	150	1.05	4.71	53	2.60
		1:1.5	180	1.04	3.59	43	1.59
		1:2	130	1.04	4.54	53	2.52
		1:2	150	1.04	4.16	51	2.23
		1:2	180	1.05	2.83	43	1.29
	CF	1:0.5	90	1.10	1.30	44	0.62
		1:0.5	120	1.09	1.56	42	0.72
		1:0.5	150	1.07	2.53	40	1.10
		1:1	90	1.10	1.43	44	0.70
		1:1	120	1.10	1.82	45	0.89
		1:1	150	1.07	2.61	43	1.21
		1:2	90	1.07	2.21	33	0.78
		1:2	120	1.07	2.35	38	0.97
		1:2	150	1.06	2.73	43	1.25
	CB	1:1	W/O	0.85	2.24	27	0.52
		1:1	90	1.05	2.68	29	0.81
		1:1	120	1.06	2.93	32	1.00
		1:1	150	1.06	3.49	35	1.30
$PC_{61}BM$	*o*-DCB	1:1	W/O	0.57	9.04	60	3.14
		1:1	90	0.57	9.17	59	3.08
		1:1	120	0.59	8.59	63	3.16
		1:1	150	0.60	9.08	61	3.34
	CF	1:1	90	0.56	6.92	54	2.09
		1:1	120	0.57	7.76	65	2.84
		1:1	150	0.58	7.70	67	3.01
	CB	1:1	W/O	0.51	5.60	46	1.32
		1:1	90	0.49	5.15	46	1.17
		1:1	120	0.49	5.88	48	1.38
		1:1	150	0.50	5.79	50	1.44

[a] Annealed for 10 min.

Figure S6. *J–V* curves of P3HT:**Cz-RH** (top) and P3HT:**Flu-RH** (bottom) films using chloroform as a solvent with various blend ratios and annealing temperatures.

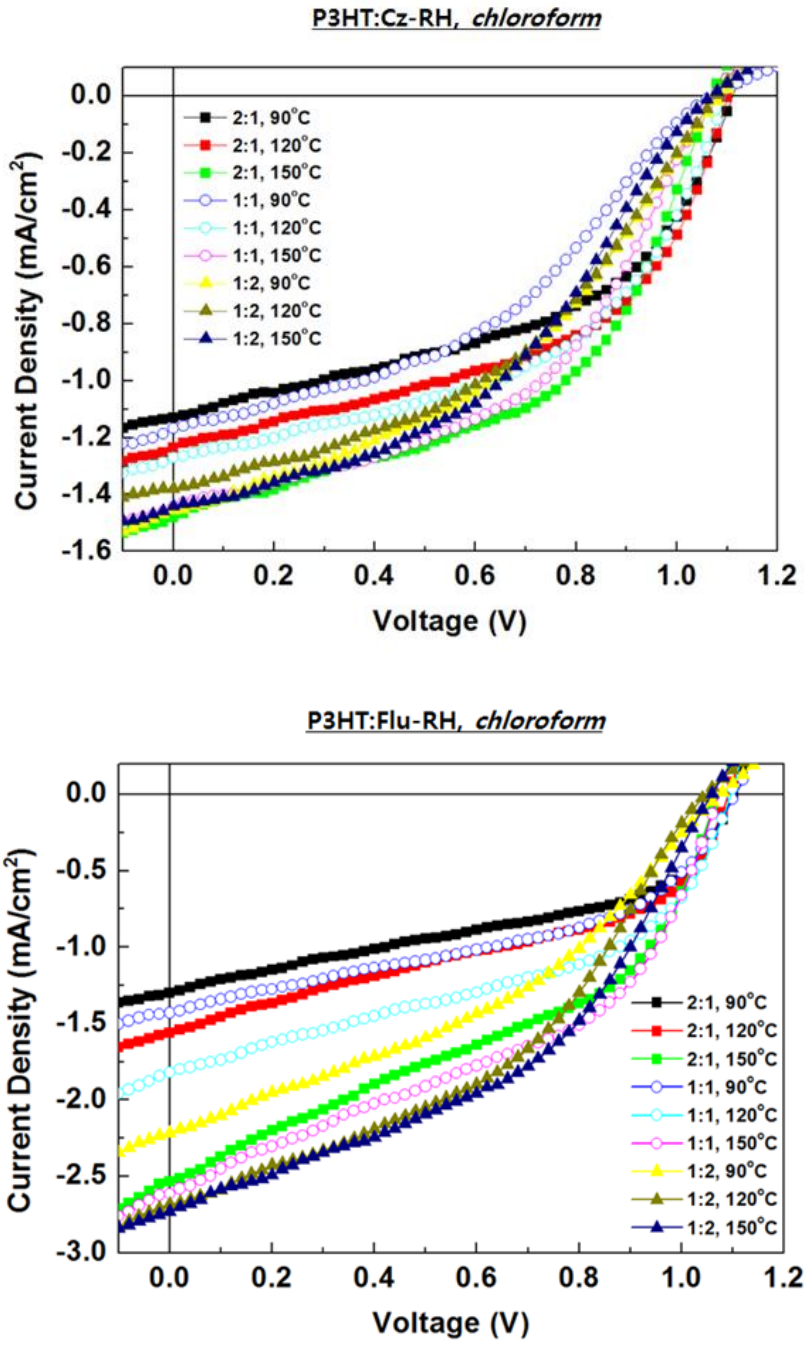

Figure S7. *J–V* curves of P3HT:**Cz-RH** and P3HT:**Flu-RH** (1:1, w/w) photovoltaic cells using chlorobenzene as a solvent with various annealing temperatures.

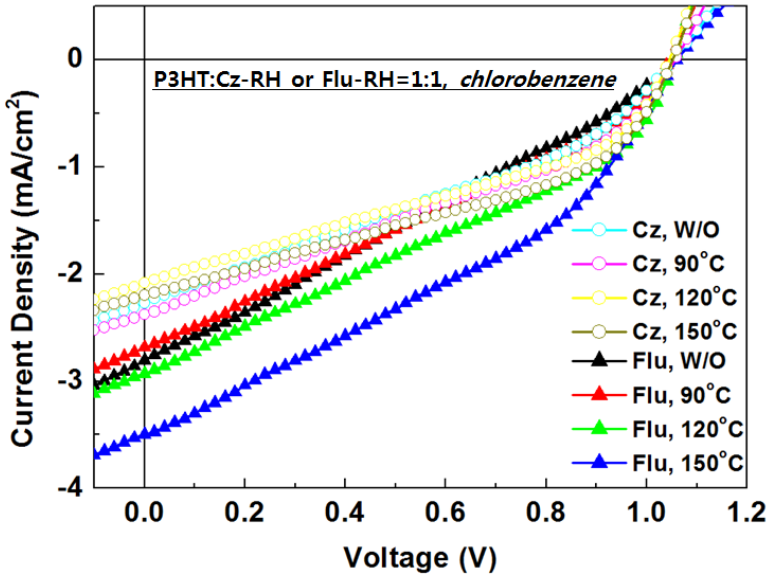

Figure S8. *J–V* curves of P3HT:**Flu-RH** photovoltaic cells using *o*-DCB as a solvent with various blend ratios and thermal annealing conditions.

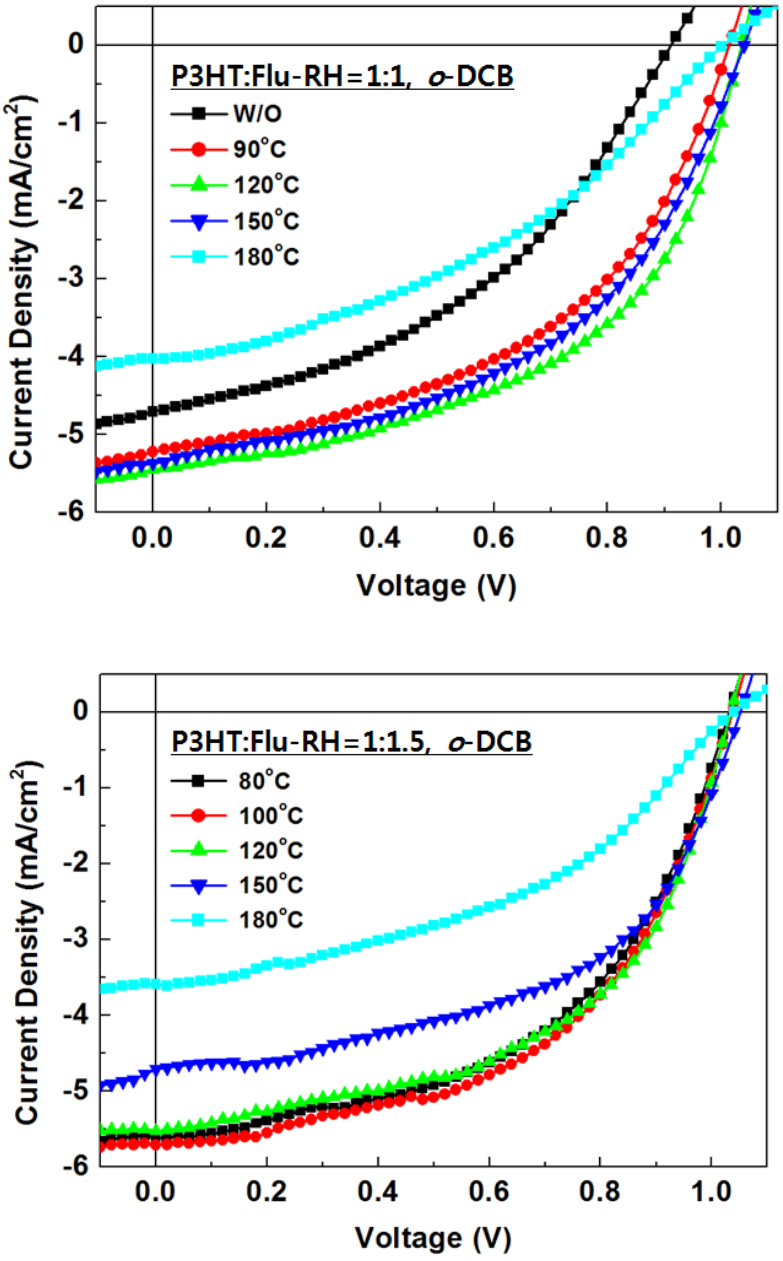

Figure S9. Selected *J–V* curves and EQE spectra of P3HT:**Cz-RH**, P3HT:**Flu-RH**, and P3HT:PCBM (1:1, w/w, chloroform (CF)).

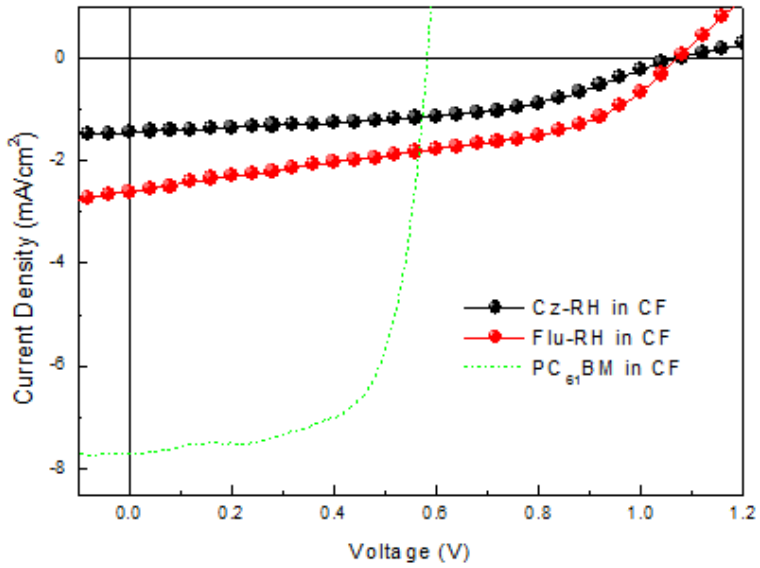

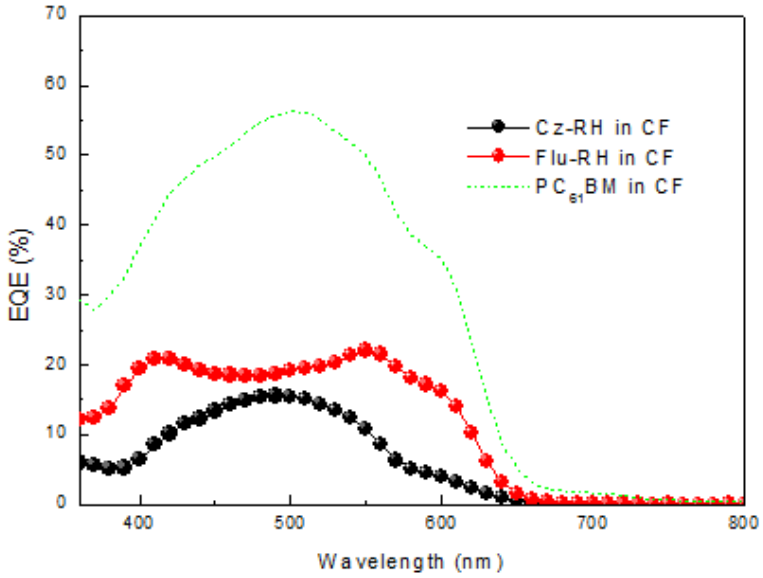

Acceptor	D–A ratio	Annealing	V_{OC}[V]	J_{SC} (mA/cm^2)	FF (%)	PCE (%)
Cz-RH	1:1 in CF	Pre 150^{o}C	1.08	1.44	47	0.74
Flu-RH	1:1 in CF	Pre 150^{o}C	1.07	2.61	43	1.21
$PC_{61}BM$	1:1 in CF	Pre 150^{o}C	0.58	7.70	67	3.01

Figure S10. Selected *J–V* curves and EQE spectra of P3HT:**Cz-RH**, P3HT:**Flu-RH** and P3HT:PCBM (1:1, w/w, chlorobenzene (CB).

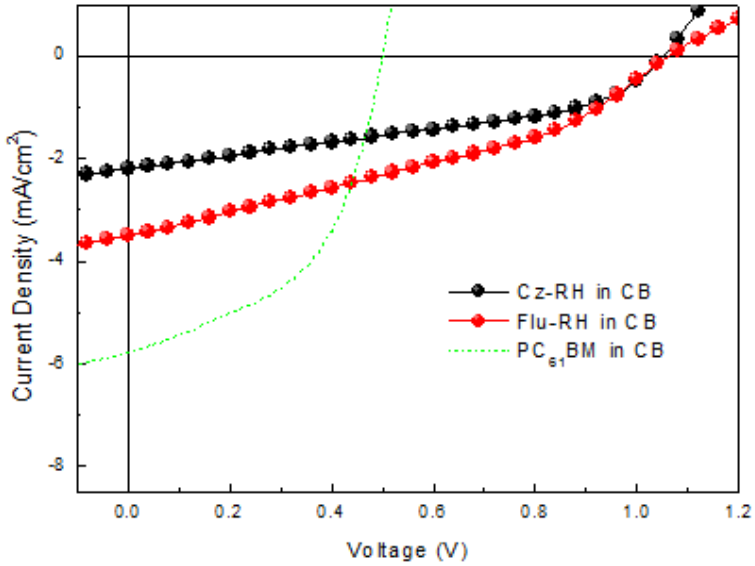

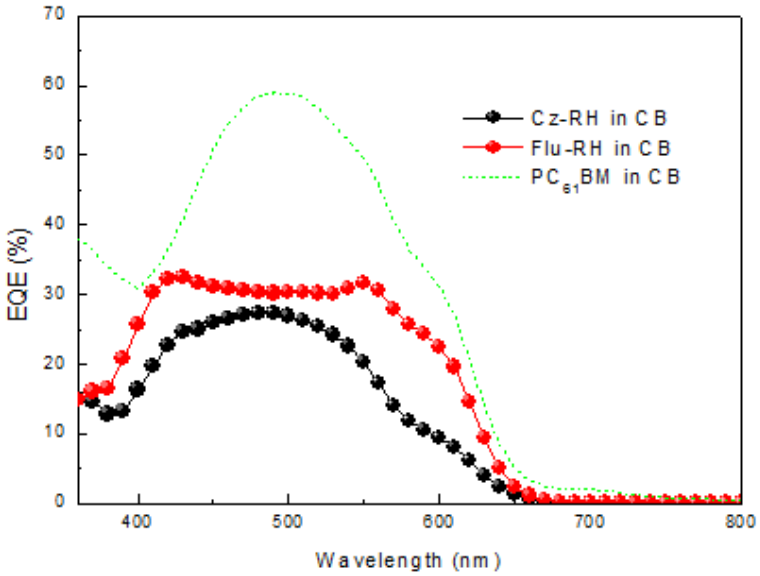

Acceptor	D–A ratio	Annealing	V_{OC}[V]	J_{SC} (mA/cm^2)	FF (%)	PCE (%)
Cz-RH	1:1 in CB	Pre 150^{o}C	1.05	2.20	41	0.94
Flu-RH	1:1 in CB	Pre 150^{o}C	1.06	3.49	35	1.30
PC$_{61}$BM	1:1 in CB	Pre 150^{o}C	0.50	5.79	50	1.44

Figure S11. Selected *J*–*V* curves and EQE spectra of P3HT:**Cz-RH**, P3HT:**Flu-RH** and P3HT:PCBM (1:1, w/w, *o*-DCB).

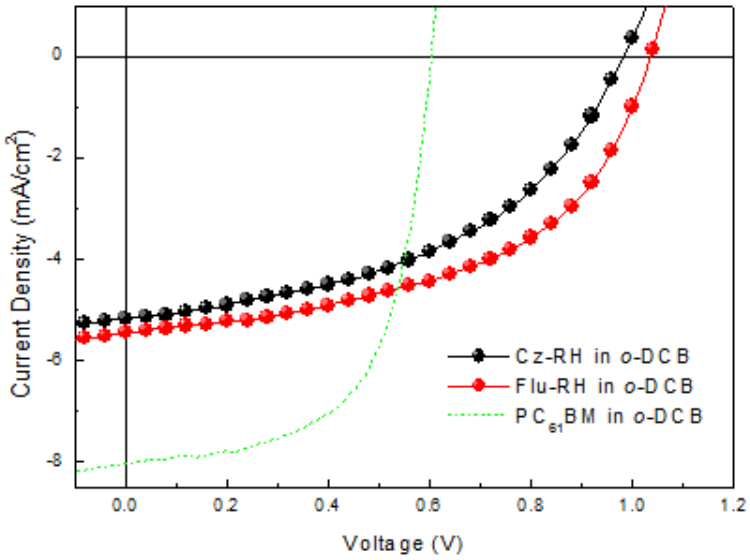

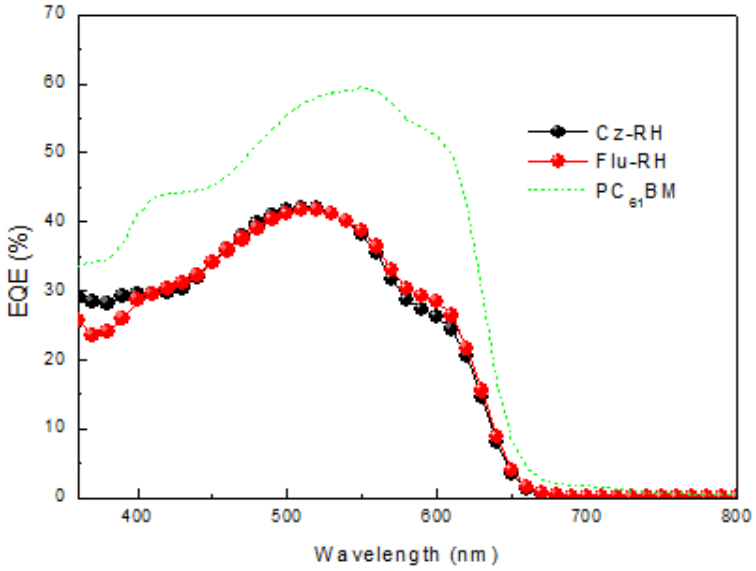

Acceptor	D–A ratio	Annealing	V_{OC}[V]	J_{SC} (mA/cm^2)	FF (%)	PCE (%)
Cz-RH	1:1 in *o*-DCB	Pre 90^{o}C	0.98	5.17	46	2.36
Flu-RH	1:1 in *o*-DCB	Pre 120^{o}C	1.04	5.44	51	2.89
$PC_{61}BM$	1:1 in *o*-DCB	Pre 150^{o}C	0.60	9.08	61	3.34

Figure S12. Selected *J*–*V* curves and EQE spectra of P3HT:**Cz-RH** and P3HT:**Flu-RH** (1:1.5, w/w, *o*-DCB).

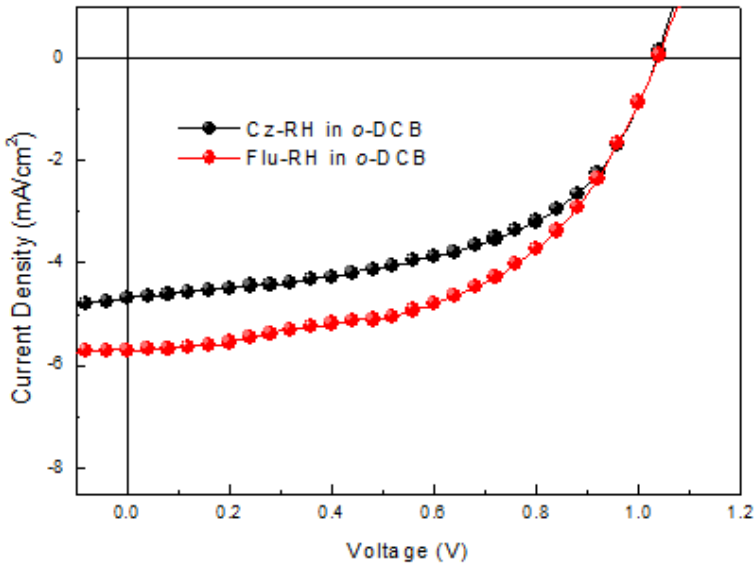

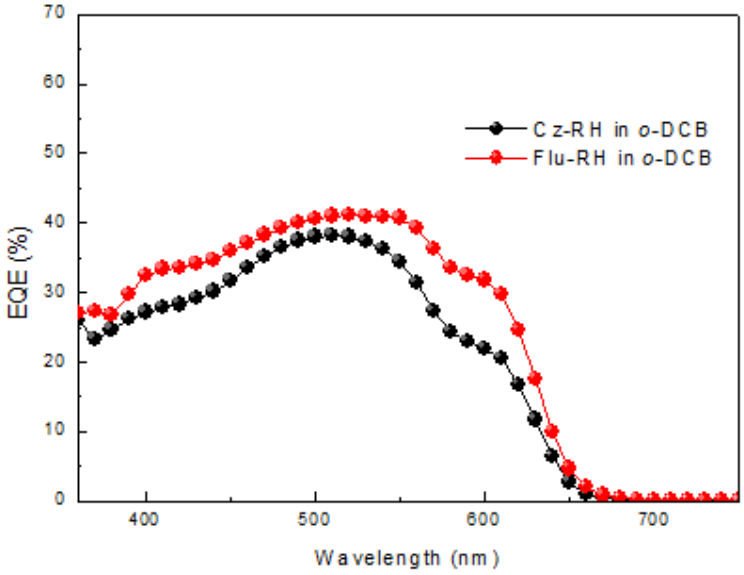

Acceptor	D–A ratio	Annealing	V_{OC}[V]	J_{SC} (mA/cm^2)	FF (%)	PCE (%)
Cz-RH	1:1.5 in *o*-DCB	Pre 100^{o}C	1.03	4.69	53	2.56
Flu-RH	1:1.5 in *o*-DCB	Pre 100^{o}C	1.03	5.70	52	3.08

7. Photoluminescence (PL) quenching experiment

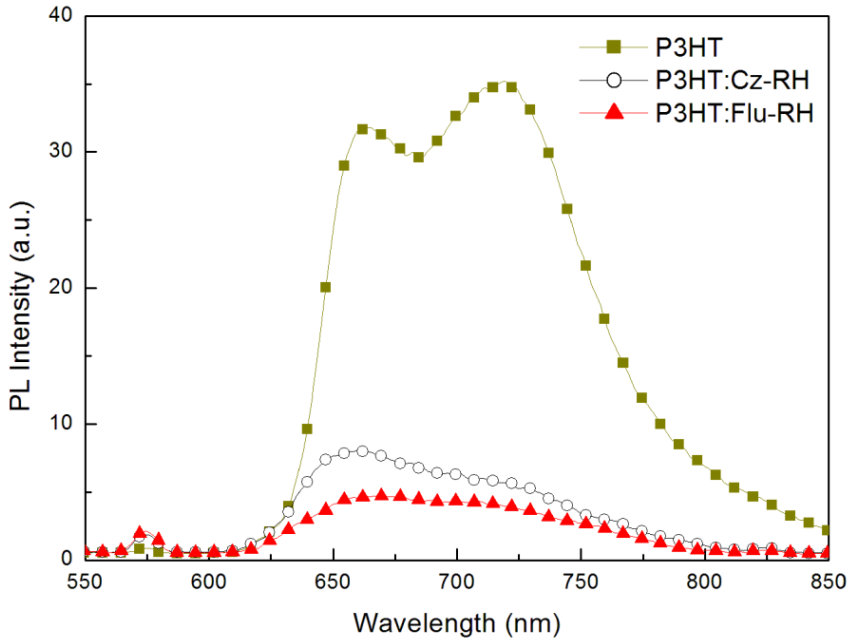

Figure S13. PL spectra of the P3HT:**Cz-RH** (1:1.5, w/w, *o*-DCB), P3HT:**Flu-RH** (1:1.5, w/w, *o*-DCB), and P3HT (*o*-DCB) films. The films were annealed at 100 ^{o}C.

8. Atomic force microscopy (AFM) images

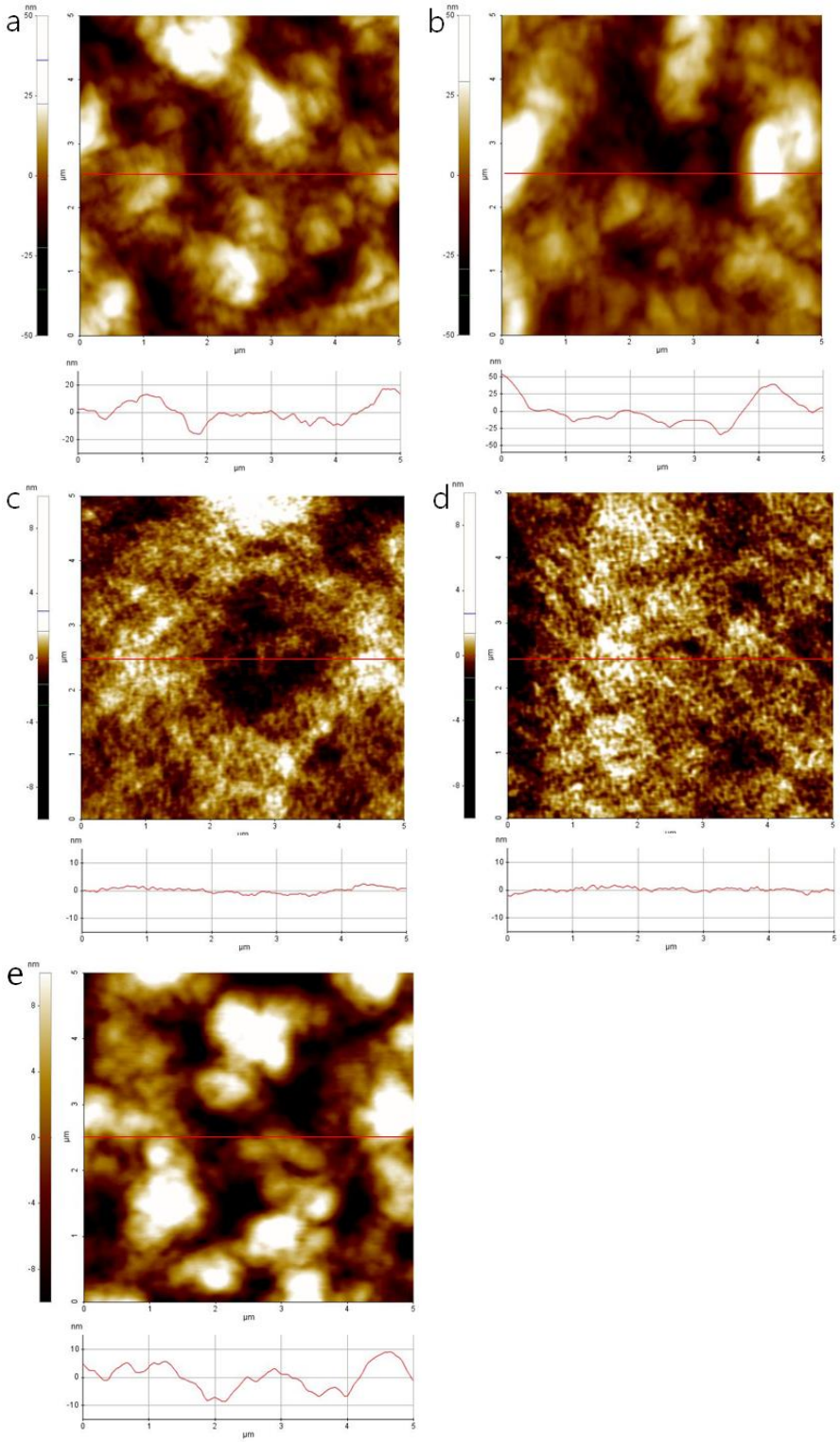

Figure S14. AFM images of the (a) P3HT:**Cz-RH** (1:1.5, w/w, *o*-DCB), (b) P3HT:**Flu-RH** (1:1.5, w/w, *o*-DCB), (c) P3HT:**Cz-RH** (2:1, w/w, chloroform), (d) P3HT:**Flu-RH** (1:2, w/w, chloroform), and (e) P3HT:PCBM (1:1, w/w, *o*-DCB) films. The films were annealed at 100^{o}C (a–b) or 150^{o}C (c–e), respectively.

9. UV absorption spectra of blend films

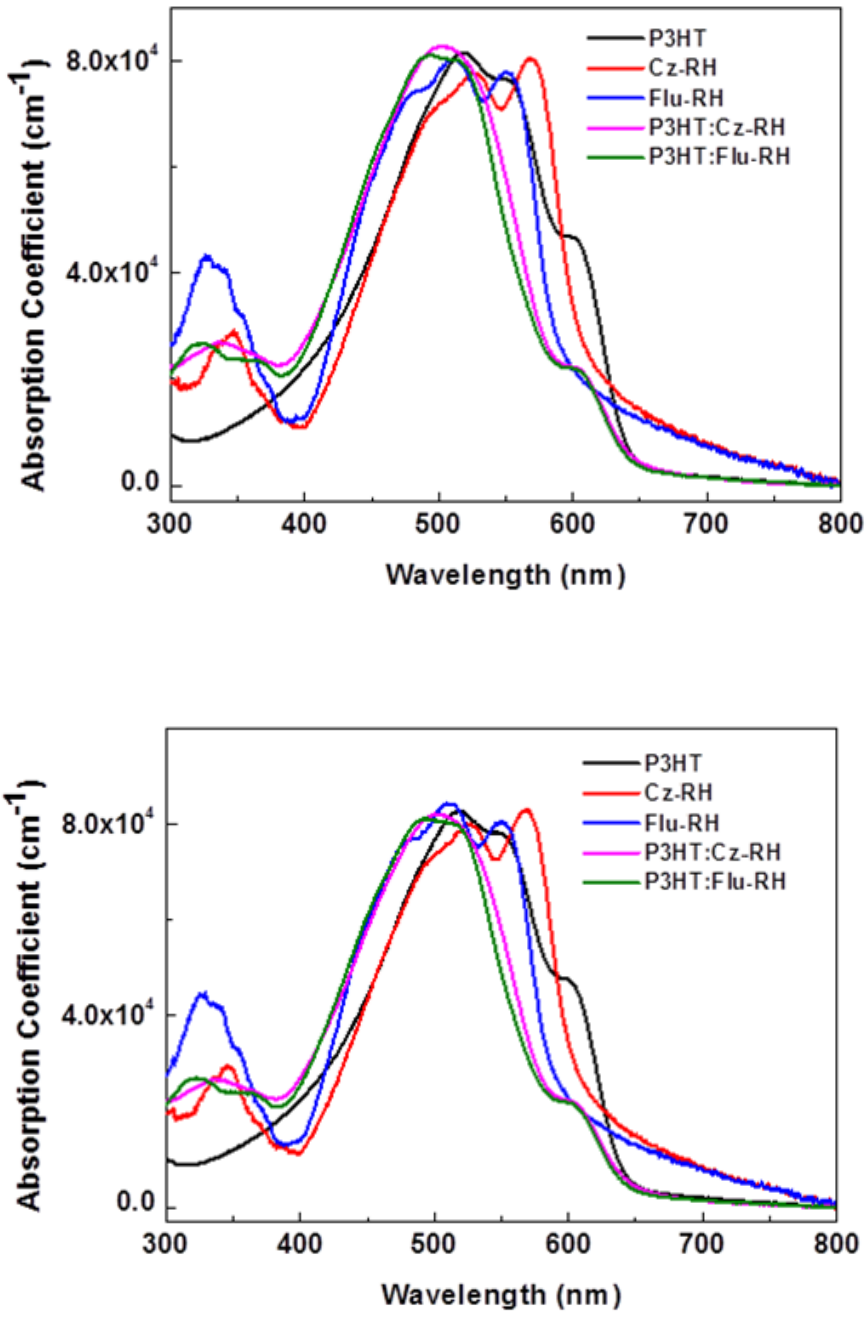

Figure S15. UV-visible absorption spectra of the as-cast (top) and annealed (bottom, at 100^{o}C, 10 min) P3HT, **Cz-RH**, **Flu-RH**, and blend films (D:A = 1:1.5, w/w, *o*-DCB).

Figure S16. Comparison of the UV-visible absorption spectra (in solid lines) and EQE (with squares) of the P3HT:**Cz-RH** and P3HT:**Flu-RH** films (1:1.5, w/w, *o*-DCB).

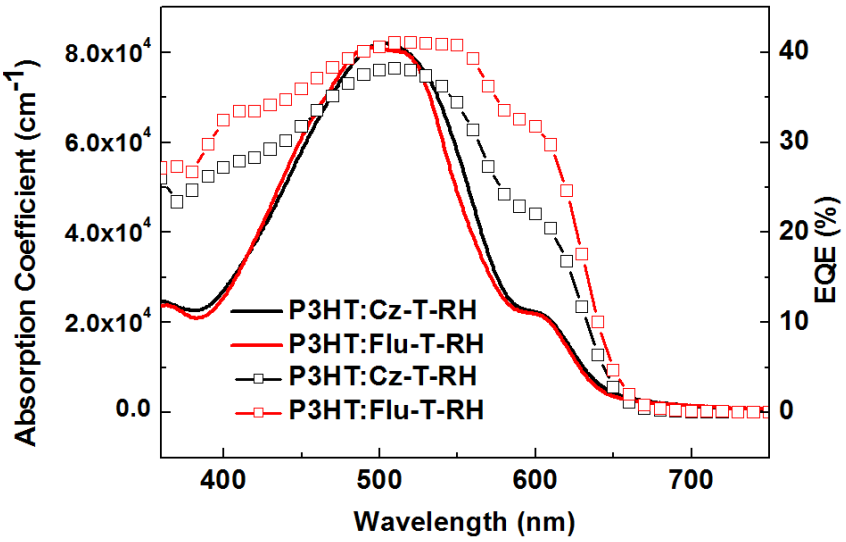

10. References

1 (a) N. Blouin, A. Michaud and M. Leclerc, *Adv. Mater.*, 2007, **19**, 2295; (b) E. Lim, B.-J. Jung and H.-K. Shim, *Macromolecules*, 2003, 36, 4288.

2 K. N. Winzenberg, P. Kemppinen, F. H. Scholes, G. E. Collis, Y. Shu, T. Birendra Singh, A. Bilic, C. M. Forsyth and S. E. Watkins, *Chem. Commun.*, 2013, **49**, 6307.

3 J. Zhou, Y. Zuo, X. Wan, G. Long, Q. Zhang, W. Ni, Y. Liu, Z. Li, G. He, C. Li, B. Kan, M. Li and Y. Chen, *J. Am. Chem. Soc.*, 2013, **135**, 8484.

4 (a) I. Grosu, G. Plé, S. Mager, E. Mesaros, A. Dulau and C. Gego, *Tetrahedron*, 1998, **54**, 2905; (b) A. N. Cammidge and K. V. L. Crépy, *J. Org. Chem.*, 2003, **68**, 6832; (c) J. Clayden, *Tetrahedron*, 2004, **60**, 4335.

5 D. M. de Leeuw, M. M. J. Simenon, A. R. Brown and R. E. F. Einerhand, *Synthetic Met.*, 1997, 87, 53.